Modelling 2016

LAN
UNIVE

Electro-mechanical-thermal Modeling of High Temperature Superconducting Cables

Yuanwen Gao, Wurui Ta, Youhe Zhou

Department of Mechanics and Engineering Sciences, College of Civil Engineering and Mechanics, Lanzhou University, Lanzhou, Gansu 730000, P.R. China

Email：ywgao@lzu.edu.cn

15 - 17 June, 2016 - Bologna, Italy

Contents

- Introduction
- Single tape modelling
- Electromechanical behavior of TSTC HTS Cable
- Electro-mechanical-thermal behavior of TSSC HTS CICC
- Conclusions

ntroduction

Superconducting Applications in Engineering

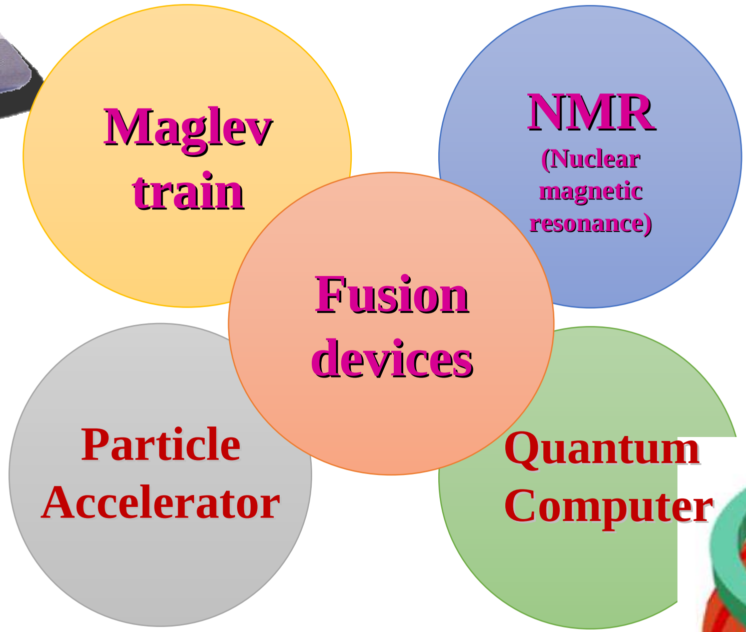

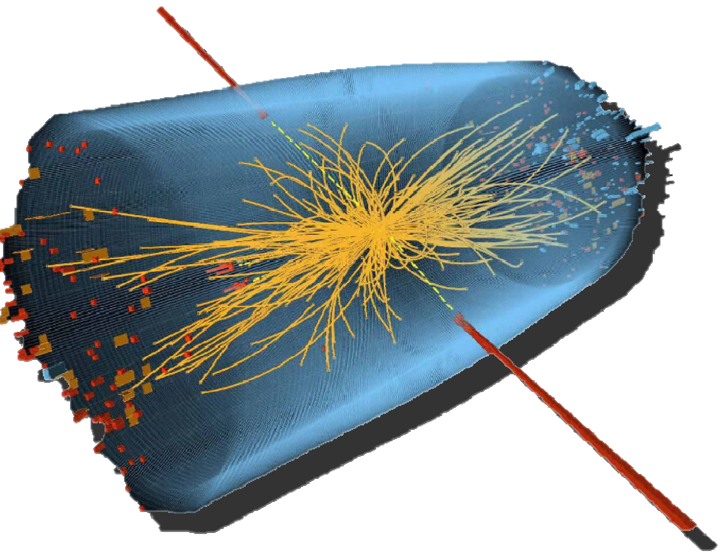

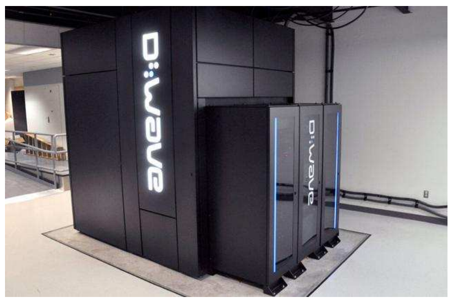

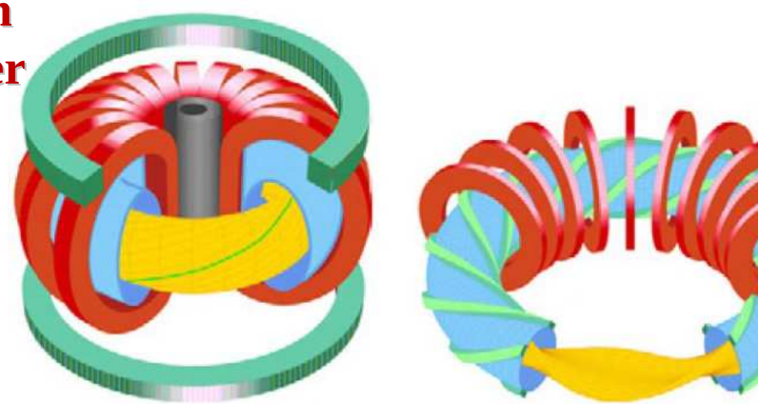

ntroduction

Superconducting Applications in Fusion devices

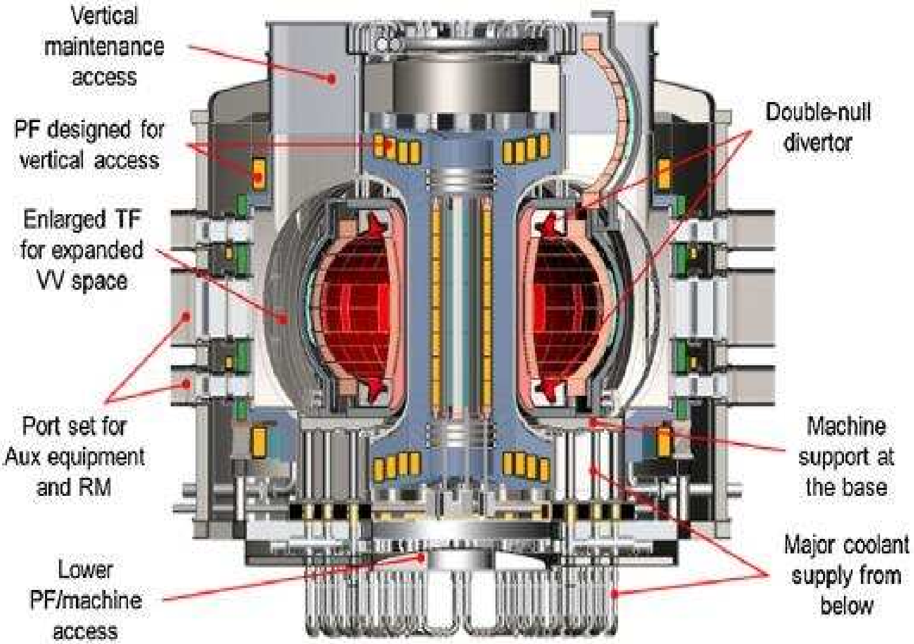

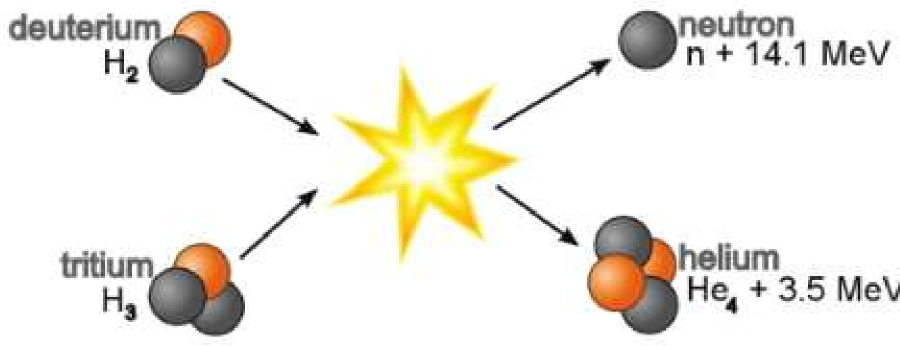

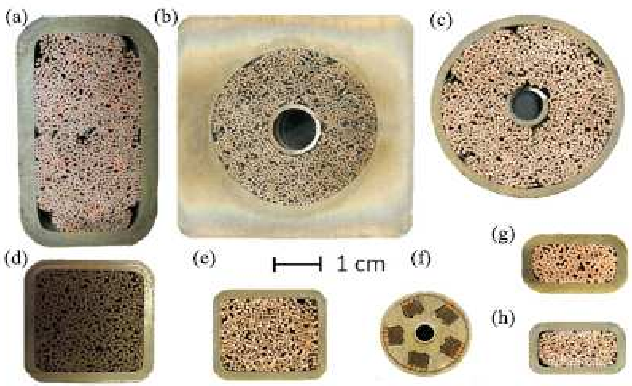

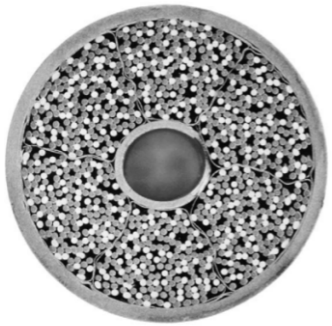

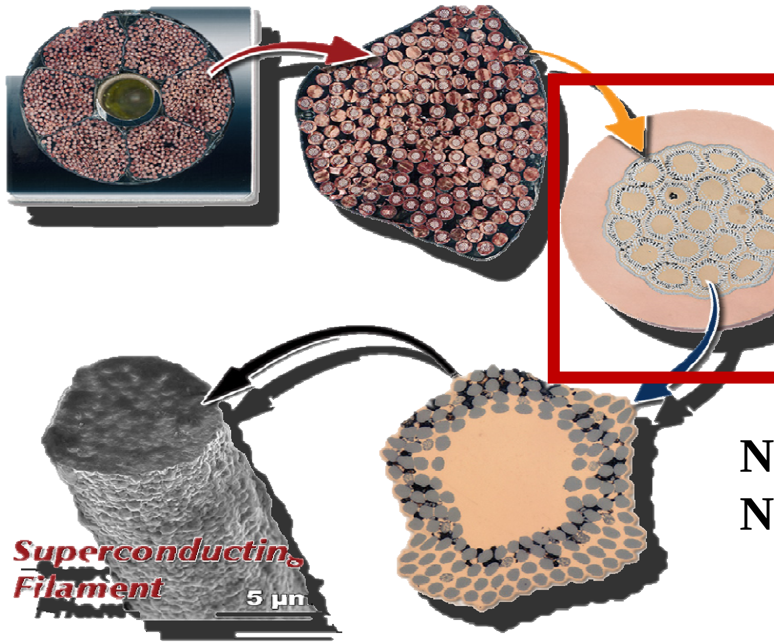

N
N

ntroduction

TSTC（twisted stacked-tape cable conductor） TSSC（twisted-stacked slotted core）HTS CICC

Compared to LTS ma ... **c heats, therma**
conductivities, and low

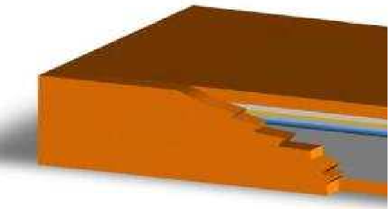

stainless stee

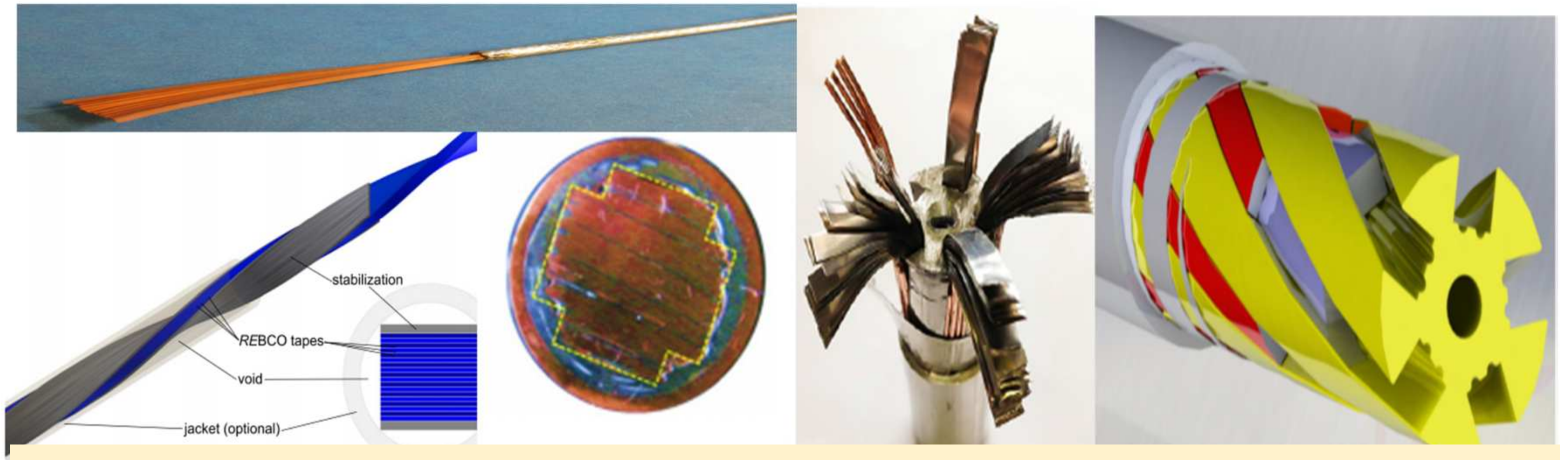

2G

material	$T_c(0)$ / K
NbTi	9.6
Nb_3Sn	18
BSCCO 2212	95
BSCCO 2223	107
REBCO	92 - 95
MgB_2	35 - 39

TSTC HTS Cable:

◆The cable consists of a stack of flat tapes twisted along the axis of the stack, and embedding the stack in single groove machined on a circular rod.

TSSC HTS CICC:

◆The HTS tapes are arranged as five ducts wound on a helically slotted Al core with an external round jacket.

◆A central channel and two semicircular grooves provide channels for coolant flow.

◆The Al core with tapes are wrapped with 50-100 μm stainless steel tape and jacketed with 1.25 mm Al foil prior to the final compaction process.

Barth C. High temperature superconductor cable concepts for fusion. 2013

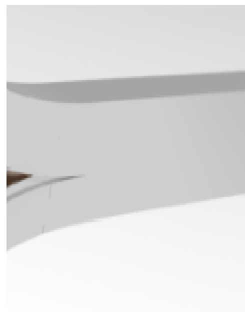

15

COR

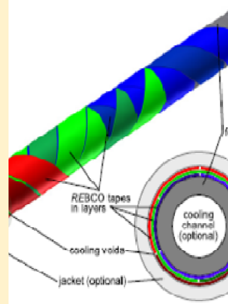

ROEBEL

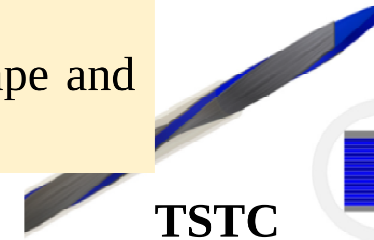

TSTC

ntroduction

Research Status-*Experiment research*

TC HTS Cable-*Electric properties*

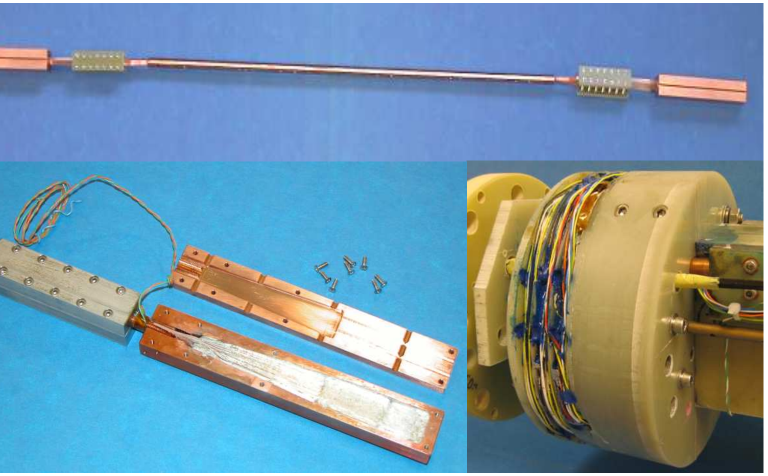

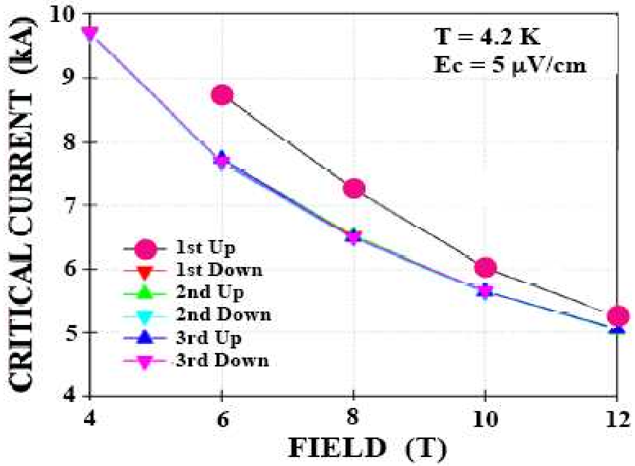

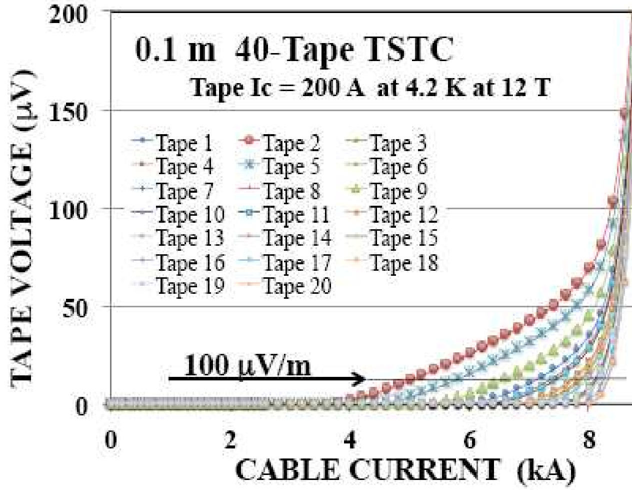

Makoto Takayasu, Luisa Chiesa, et. al. Present Status and Recent Developments of the Twisted Stacked-Tape Cable (TSTC) Conductor. 2015

C HTS CICC-*Electric properties*

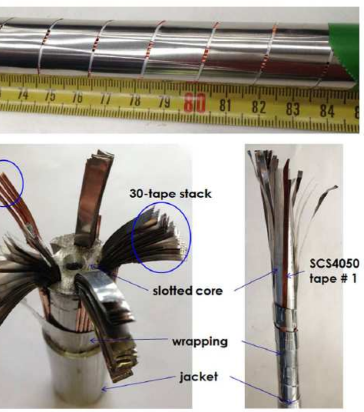

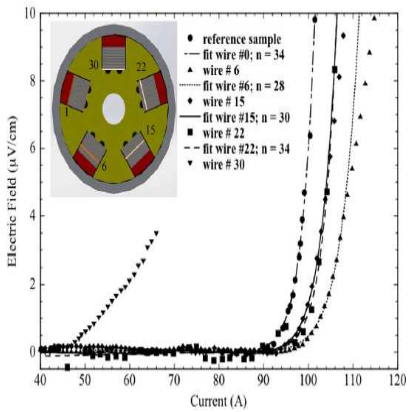

G. Celentano, G. De Marzi.et.al. ,2014

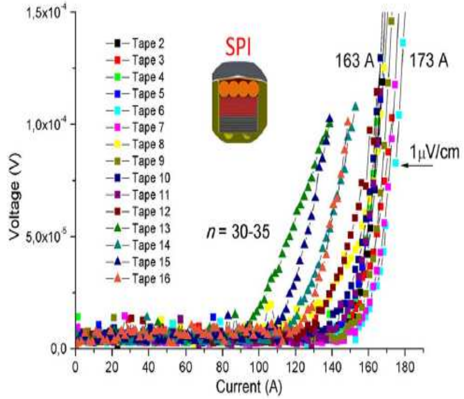

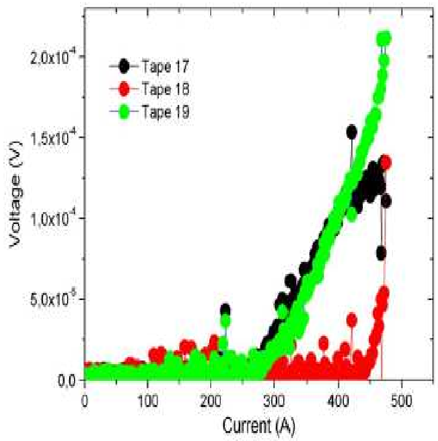

A. Augieri, G. De Marzi.et .al., 2015

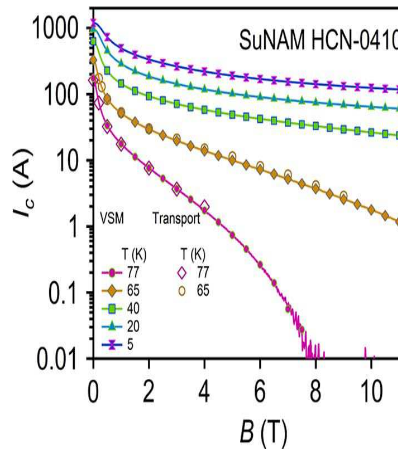

Gianluca De Marzi, Giuseppe Celentano. et.

ntroduction

Research Status-*Numerical simulation*

STC HTS Cable-*Temperature-and field dependent characterization*

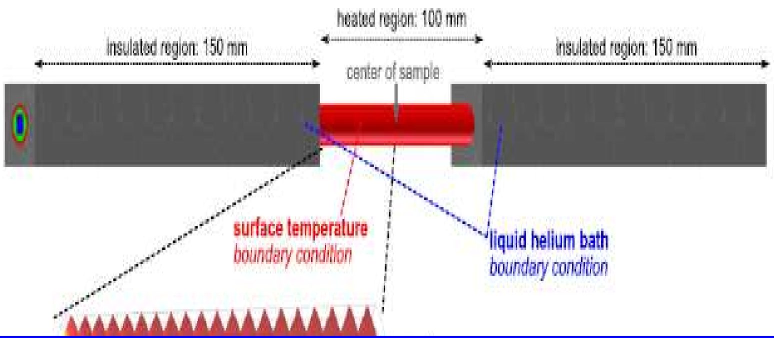

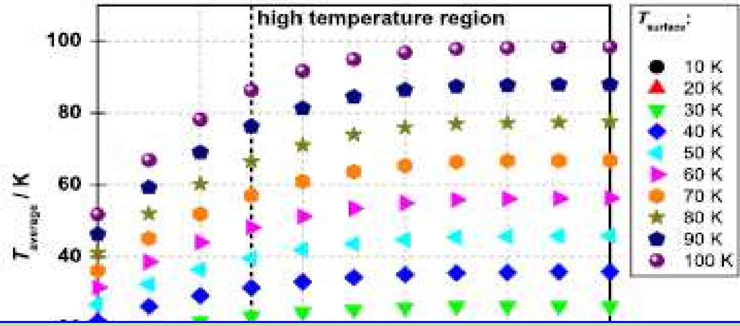

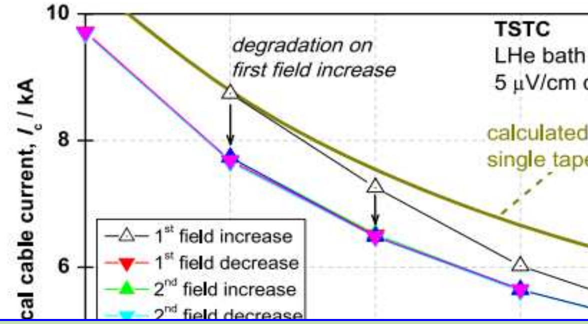

Although some works have already carried out, the related research has just started, more 3D models are still very required.

SSC HTS CICC-*Structural modelling*

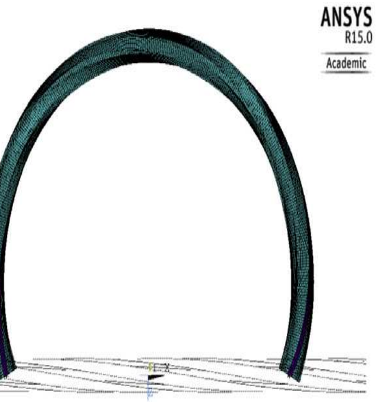

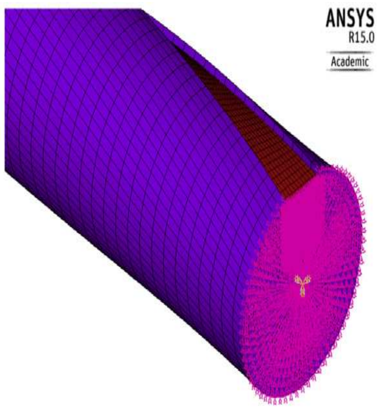

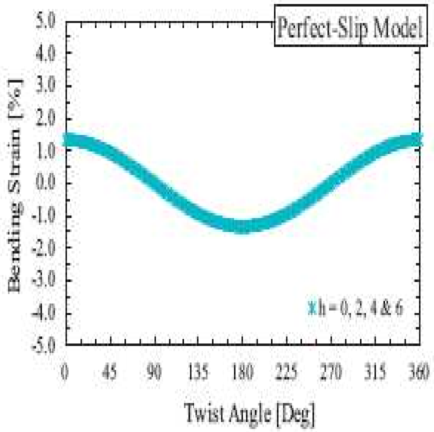

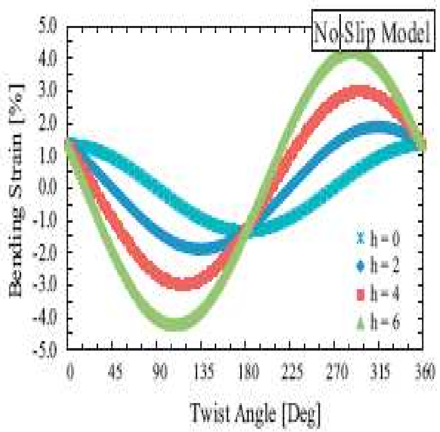

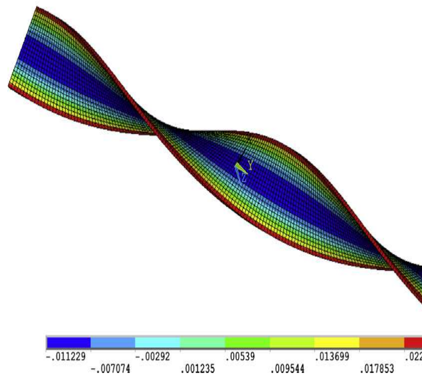

N.C. Allen, L. Chiesa, M. Takayasu Structural modeling of HTS tapes and cables. Cryogenics.2016

Gianluca De Marzi, Giuseppe Celentano. et.

ngle tape modelling

LAN
UNIVE

The structure diagram of 2G coated conductors： Tape

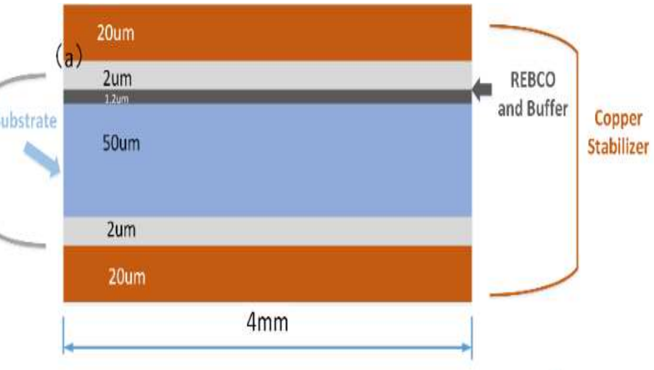

	Copper Stabilizer	Silver overlayer	Substrate	REBCO/ Buffer
E(GPa)	350	90	180	150
T(GPa)	4	22	7.5	-
Y(MPa)	85	225	1225	-

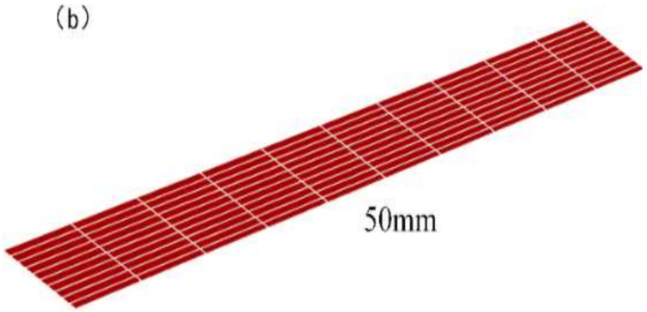

Mesh

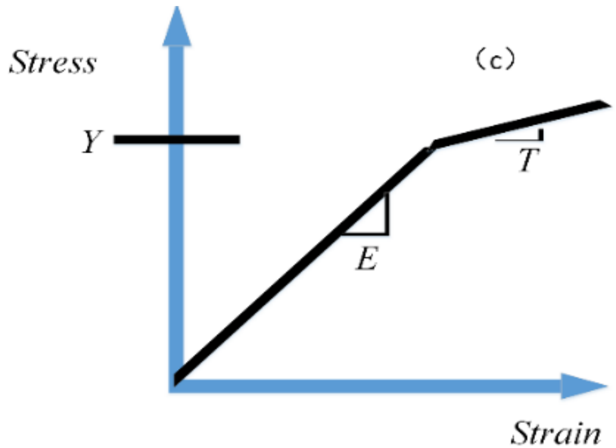

Bilinear isotropic hardening material model

Mesh consists of 1350 domain elements, 1935 boundary elements, and 444 edge elements. The bilinear properties for each elastic-plastic material were taken from stress–strain data at 77 K.

Finite Element Equation

$$K_{ep}(\mathbf{a})\mathbf{a} = \mathbf{Q}$$

Iterative process:

1. Forming the elastic stiffness matrix ***Ke***。

2. Solving elasticity problem

   $\mathbf{a}^{(1)} = \boldsymbol{K_e}^{-1}\mathbf{Q}$ (n=1,2…)

3. Calculate the equivalent strain of every Gauss integra points。

4. $\sigma_s - \bar{\varepsilon} \longrightarrow \sigma_s(\bar{\varepsilon}^{(n)})$

5. Calculate the elastic shear modulus of every G integration points

6. Forming the plastic stiffness matrix ***Kp*** *(n)*

7. Solving plastic problem

   $\mathbf{a}^{(n+1)} = (\boldsymbol{K_{ep}}^{(n)})^{-1}\mathbf{Q}$

8. Check convergence $\dfrac{\left\| a^{(n+1)} - a^{(n)} \right\|}{\left\| a^{(n+1)} \right\|} \le er$

9. Output

ngle tape modelling

Mesh independence verification

Meshing way	displacement（um）（relative error）	stress（Pa）（relative error）	strain (relative error)
5×5×6	6.0413	9.8564×10^{7}	1.8058×10^{-4}
10×10×6	6.1533（1.853%）	9.9245×10^{7} (0.690%）	1.7948×10^{-4} (0.609%）
15×15×6	6.1880（0.563%）	9.9457×10^{7} (0.213%）	1.7918×10^{-4} (0.167%）
20×20×6	6.2048（0.271%）	9.9559×10^{7} (0.102%）	1.7903×10^{-4} (0.0837%）

Stress-strain curve of superconducting tapes

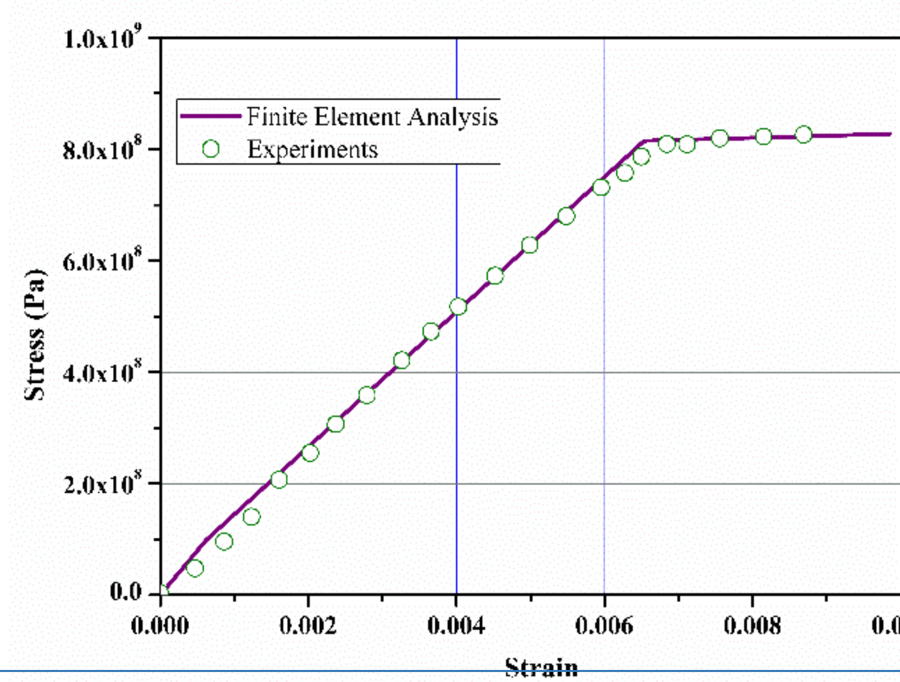

- Copper layer and the base layer has a significant effect on the mechanical behavior of the whole superconducti tapes，and the impact of REBCO and the buffer layer can be ignored.
- The yield limit, Young's modulus and tangent modulus of superconducting tape are 810 MPa, 131GPa, and 3.78GPa, respectively.
- the electric and thermal parameters of tapes employed in our simulations are directly from experimental data

ectromechanical behavior of TSTC HTS Cable

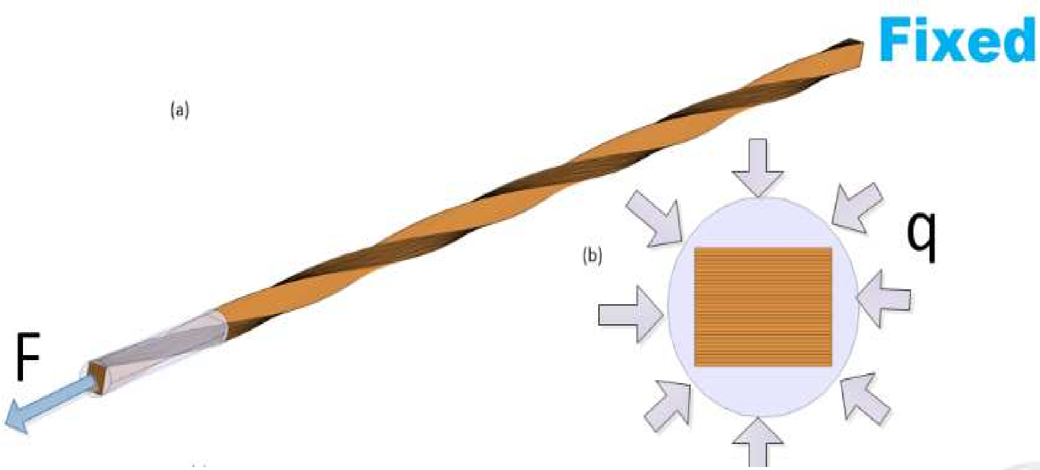

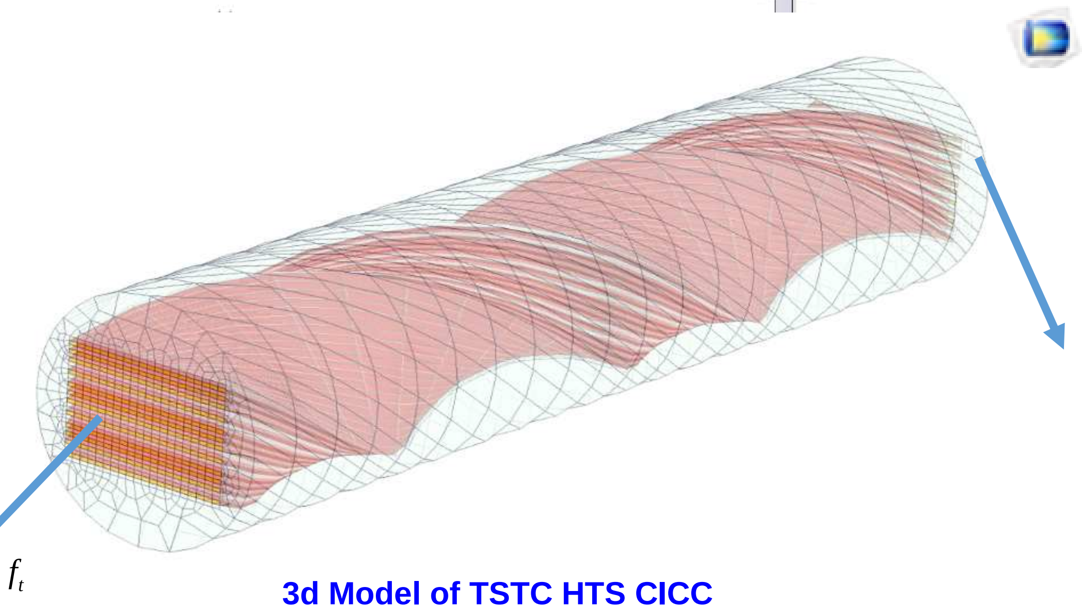

$$\begin{bmatrix} u_s \\ v_s \\ w_s \end{bmatrix} = \begin{bmatrix} 0 \\ 0 \\ 0 \end{bmatrix}$$

3d Model of TSTC HTS CICC

Domain	Taps	Jacket and Embedding Material	Total
Element number	12000	2790	14790

Simulation steps:

- Select the type of shape function element
- Build 3D geometric model of the TSTC HTS Cable
- Divide the finite element mesh
- Set the boundary conditions
- Solve equations using iterative method
- Check mesh independence

ectromechanical behavior of TSTC HTS Cable

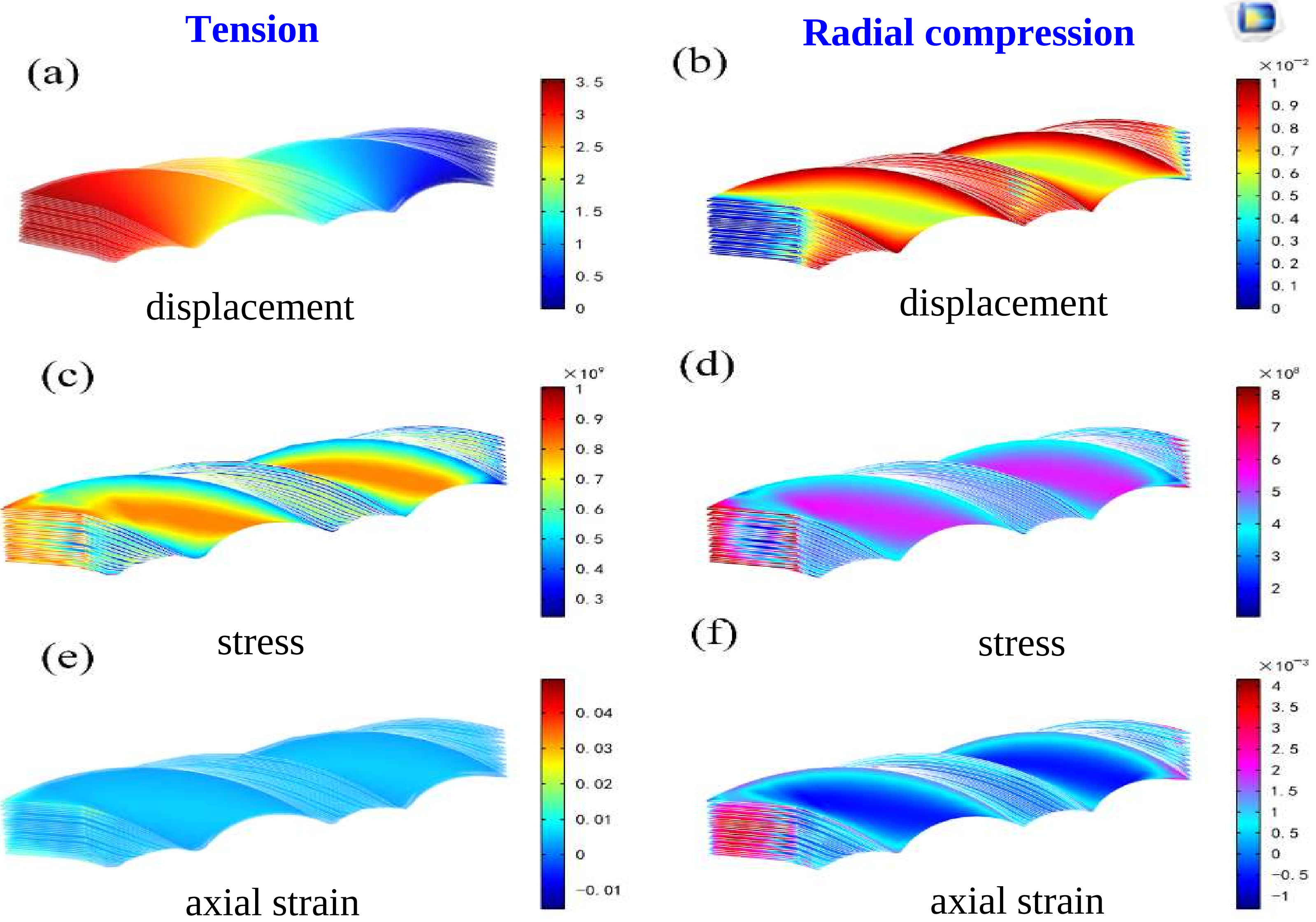

Distribution of displacement, stress and axial strain in taps.

Tension:

- The displacement gradually increasing along the axial direction. The maximum value occurs at one end applied the tension force, and the other end is zero.
- The stress of taps located in middle of stack is larger than i edge, and the axial strain in the stack is uniformly distributed.

Radial compression:

- The displacement and axial strain of taps located in the edg of stack are larger than in midd
- The stress of taps located in the middle of stack is larger th in edge

ectromechanical behavior of TSTC HTS Cable

LAN
UNIVE

ritical current degradation

$$J_c(\varepsilon_{\text{axial}}) = J_{c0}(1 + a_1\varepsilon_{axial} + a_2\varepsilon^2_{axial} + a_3\varepsilon^3_{axial} + a_4\varepsilon^4_{axial} + a_5\varepsilon^5_{axial} + a_6\varepsilon^6_{axial})$$

Makoto Takayasu et. al. AIP Conference proceding,2010

$$I_c = \sum_{n=1}^{40} \mathrm{t} \int_{-\frac{w}{2}}^{\frac{w}{2}} J_c^{(n)}(\varepsilon_{\text{axial}})dS$$

Tension

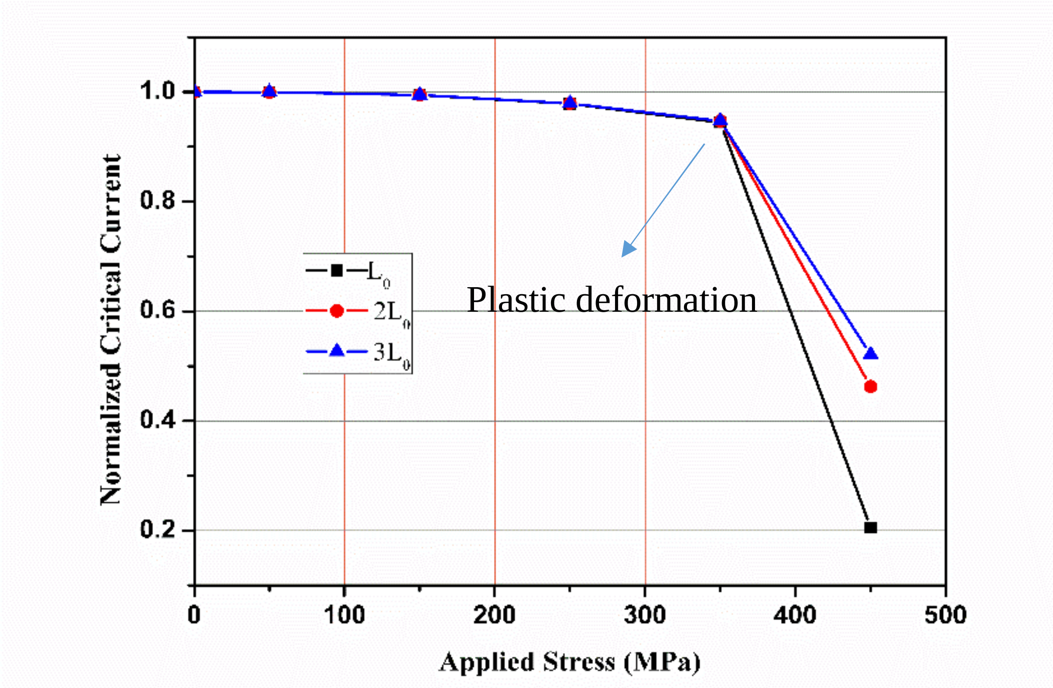

Radial compression

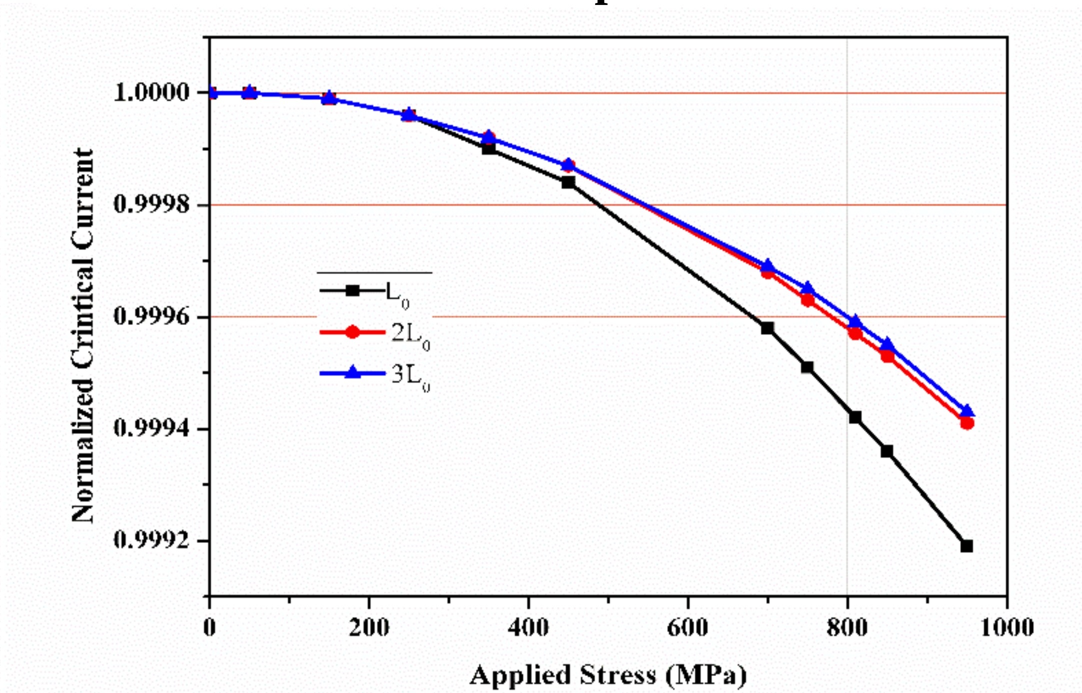

- Both in tension and radial compression cases, the critical current decreases with increasing load.
- The plastic deformation makes the degradation more obvious.
- Compared to the short twist pitch cable, the degradation of longer twist pitch cable is smaller.

tro-mechanical-thermal behavior of TSSC HTS CICC

LAN
UNIVE

Numerical Model

Characteristics:

- **3D Modelling**
- **multi-field interaction**
- **Electromagnetic characteristics**
- **Thermo-Mechanical characteristics**

3D FEA model in COMSOL Multiphysics

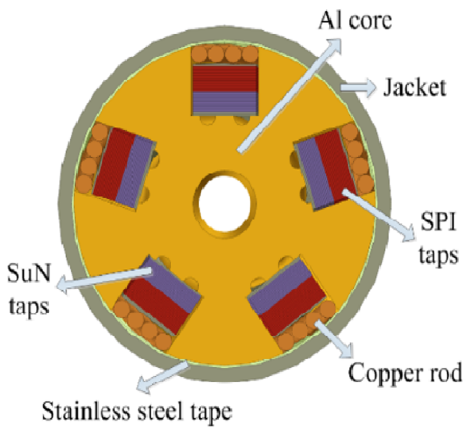

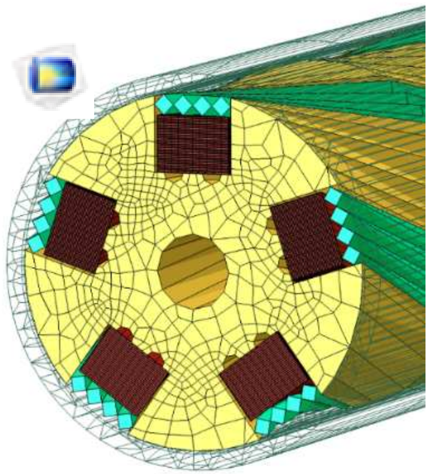

Basic equations

Electromagnetism Equations

$$\nabla\times\mathbf{E}=-\mu\frac{\partial\mathbf{H}}{\partial t}$$

$$\nabla\times\mathbf{H}=\mathbf{J}$$

$$\nabla\cdot\mathbf{H}=\mathbf{0}$$

$$\mathbf{J}=\sigma_s\mathbf{E}$$

$$\sigma_s=\frac{J}{E}=\frac{J_c(\varepsilon)^n}{E_c}J^{1-n}$$

$$\begin{bmatrix}H_{x0}\\H_{y0}\\H_{z0}\end{bmatrix}=\begin{bmatrix}f_{x0}(\mathrm{t})\\f_{x0}(\mathrm{t})\\f_{y0}(\mathrm{t})\end{bmatrix}$$

$$I_0=\int_s\mathbf{J}\cdot\mathbf{n}ds$$

$$\mathbf{n}\times(\mathbf{H}_1-\mathbf{H}_2)=\mathbf{0}$$

multi-field coupling

Mechanics Equations

$$(\lambda+\mathrm{G})\frac{\partial\Theta}{\partial x}+G\nabla^2u-2G\alpha\frac{\partial\Delta T}{\partial x}+f_x=0,$$

$$(\lambda+\mathrm{G})\frac{\partial\Theta}{\partial y}+G\nabla^2v-2G\alpha\frac{\partial\Delta T}{\partial y}+f_y=0,$$

$$(\lambda+\mathrm{G})\frac{\partial\Theta}{\partial z}+G\nabla^2w-2G\alpha\frac{\partial\Delta T}{\partial z}+f_z=0.$$

$$u=0,\ v=0,\ w=0.$$

Heat Conduction Equation

$$\rho C_p(T)\frac{\partial T}{\partial t}+\rho C_p(T)\mathbf{u}\cdot\nabla T=\nabla\cdot(k(T)\nabla T)+\mathbf{E}\cdot\mathbf{J}$$

$$k(T)\nabla T=h(T)(T_s-T_0)\qquad k(T)\cdot\square T=0$$

ctro-mechanical-thermal behavior of TSSC HTS CICC

$$I_0 = \int_s \mathbf{J}\cdot\mathbf{n}ds, (I_0 = I_e \sin(2\pi ft))$$

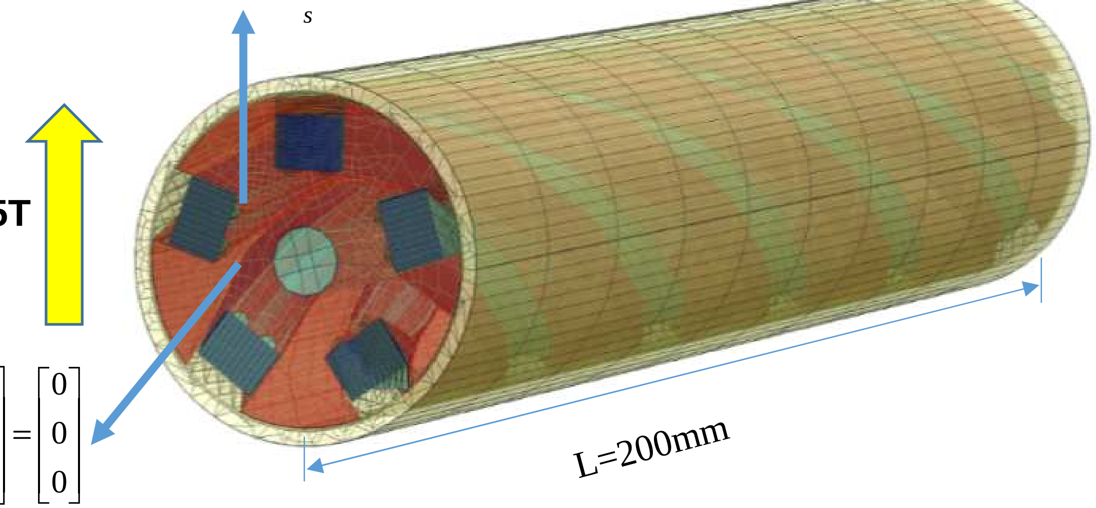

$$= \begin{bmatrix}0\\0\\0\end{bmatrix}$$

3d Model of TSSC HTS CICC

Mesh

ain	Taps	Al core	Copper rods	stainless steel tape	Al foil	Air	Total
ent ber	15000	19470	19670	20930	22780	18470	116320

Edge element

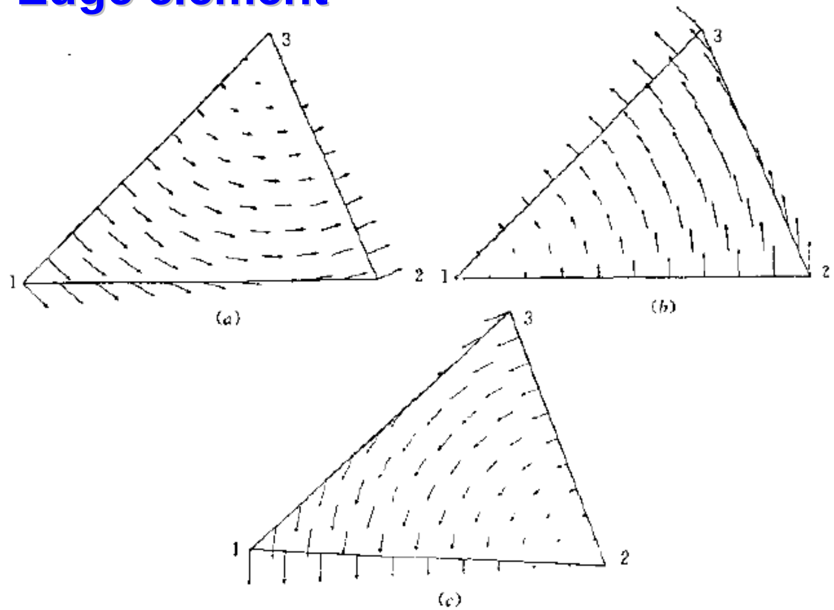

vector basis function（a）N_1^e (b) N_2^e (c) N_3^e

$$N_j^e(\mathrm{x})\cdot \mathrm{t}_j = 1\ (\mathrm{x}\in j-\mathrm{edge})$$

$$N_j^e(\mathrm{x})\cdot \mathrm{t}_k = 0\ (\mathrm{x}\in \textit{other edge})$$

$$\nabla\cdot N_j^e(\mathrm{x}) = 0 \rightarrow \nabla\cdot\mathbf{H}=\mathbf{0}$$

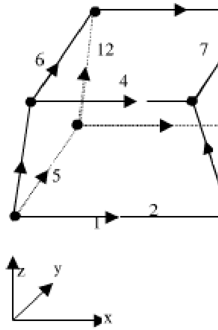

tro-mechanical-thermal behavior of TSSC HTS CICC

rrent distribution

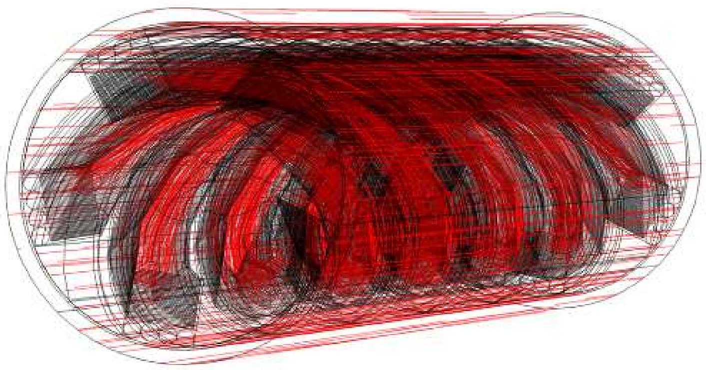

rrent streamline with its concentration on taps, t=0.005s,*Ie*=20kA, *f*=50Hz

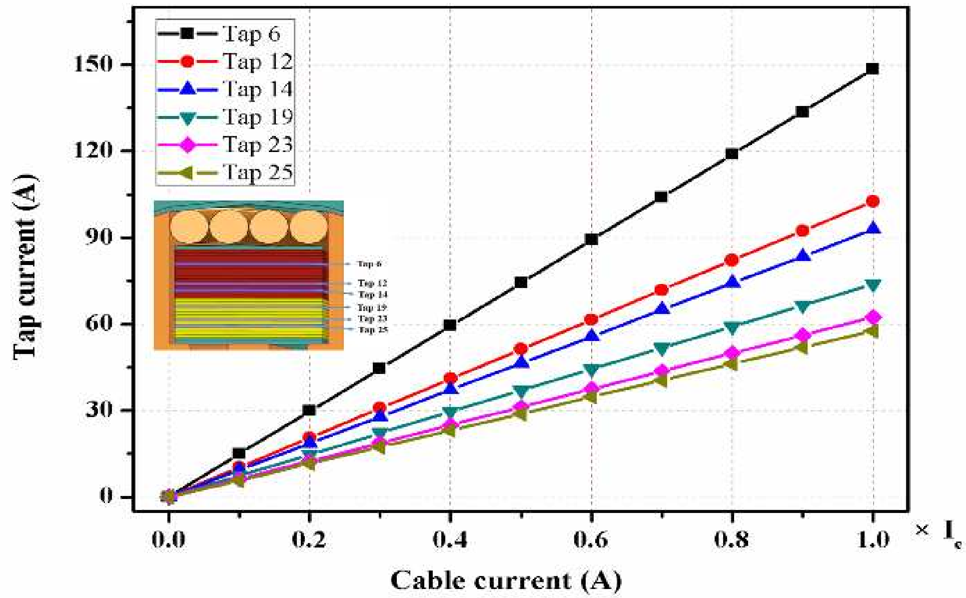

The current in different taps increase as the cable current increases

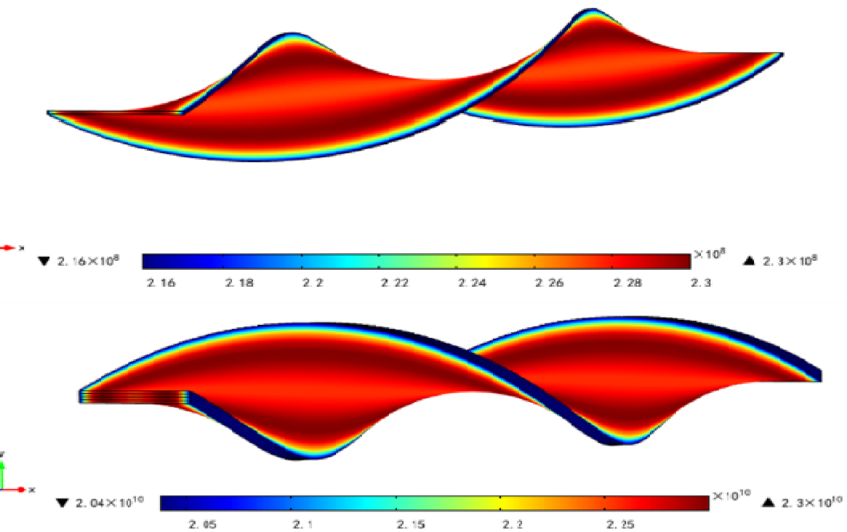

The current density distribution on Sun taps，t=0.005s,*Ie*=20kA, *f*=50Hz

- The current is concentrated mostly on the superconducting taps and the streamlines more likely coincide with the tap trajectories.
- Since the maximum strain occurs at the edge of taps, so the current density at the edges is minimized.
- The transport current is non-uniformly distributed among the 150 tapes, the current decrease from the top tape in the stack to the bottom.
- we can arrange taps with different critical current from bottom to top to improve the transport performance of the cable.

LAN
UNIVE

ctro-mechanical-thermal behavior of TSSC HTS CICC

agnetic field distribution

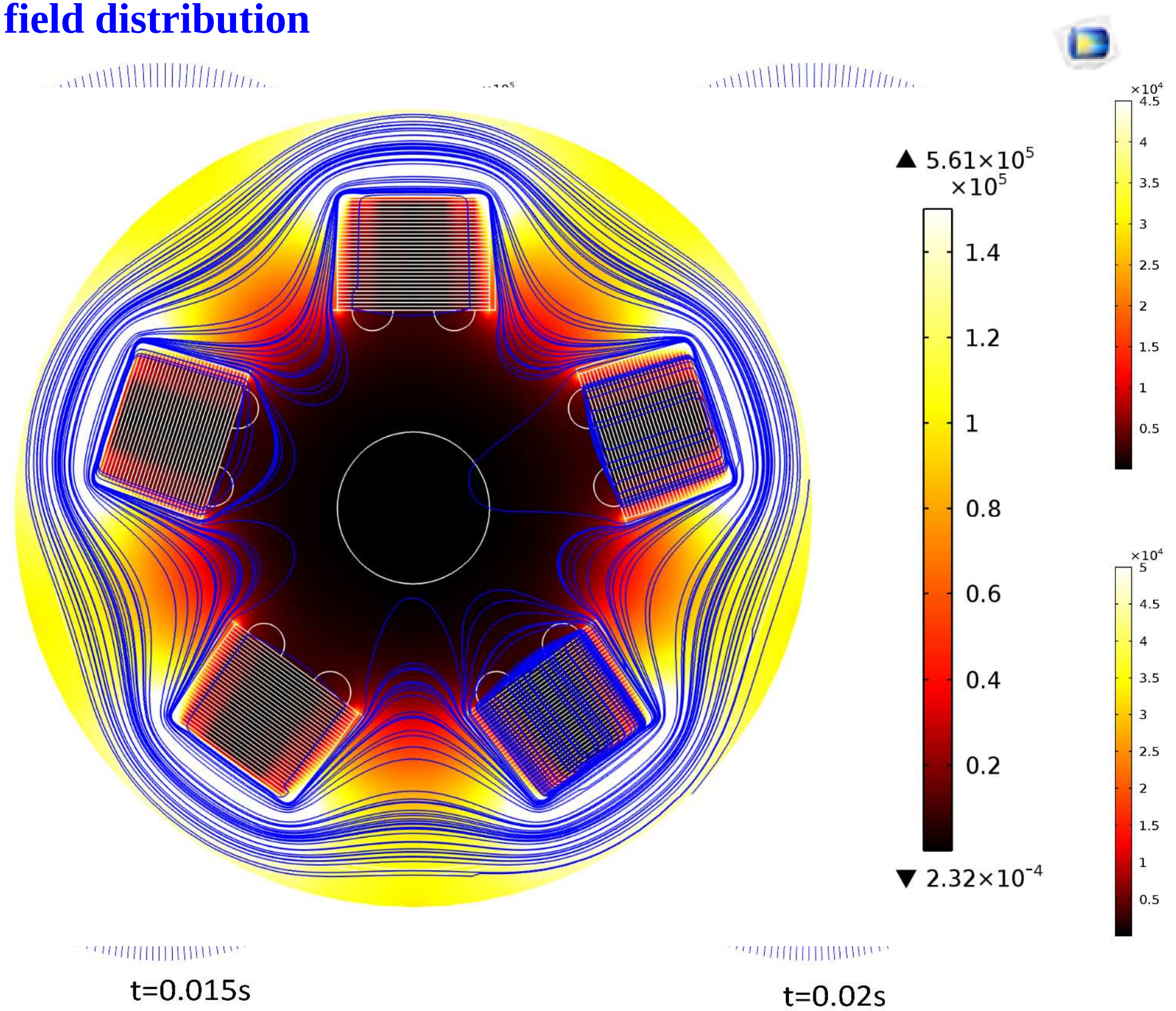

ransient magnetic field distribution on the middle cross section of cable for four time points. *Ie*=20kA, *f*=50Hz

- The cable is placed in an 15T external magnetic field and carr transport current whose amplitu is 20kA and varying with time a a sine wave. *f=50* Hz.
- Harmonic change with time in th transport current causes corresponding variations of the magnetic field at the same frequency.
- The magnetic field penetrates in the outer shell of cable and the taps almost expels the magnetic field.

ctro-mechanical-thermal behavior of TSSC HTS CICC

LAN
UNIVE

characteristic

Experimental data from Reference "A. Augieri, et. al. Electrical Characterization of ENEA High Temperature Superconducting Cable,2015"

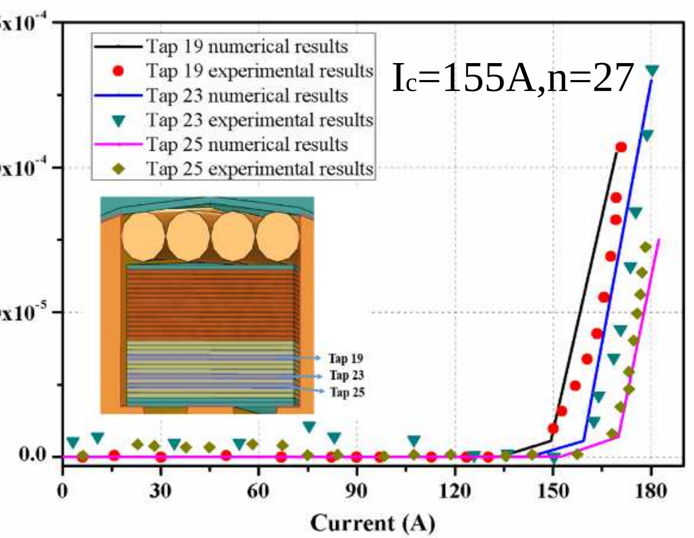

$$V = L\int_S E_z ds / S$$

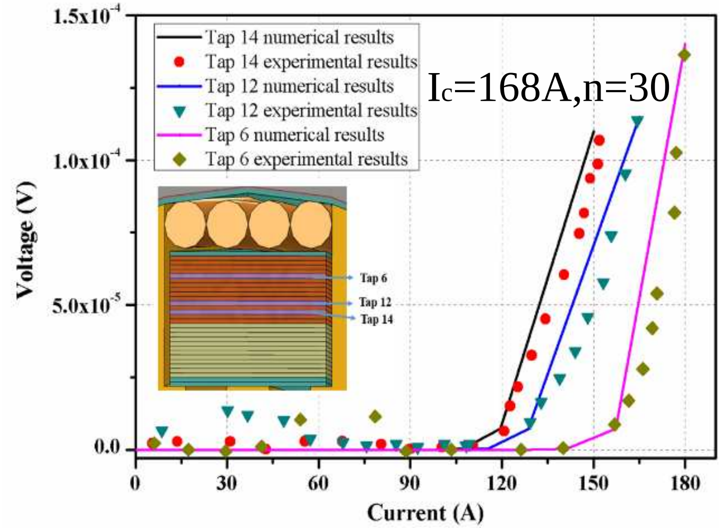

Loss

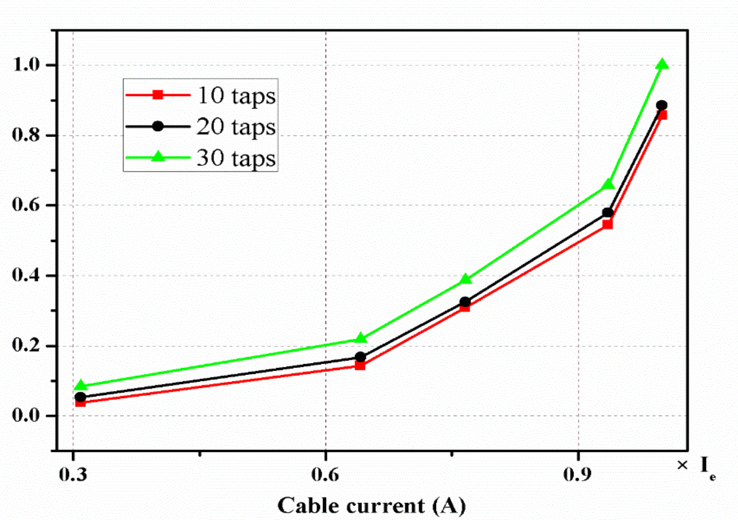

$$Q = \int_V J \cdot E dv$$

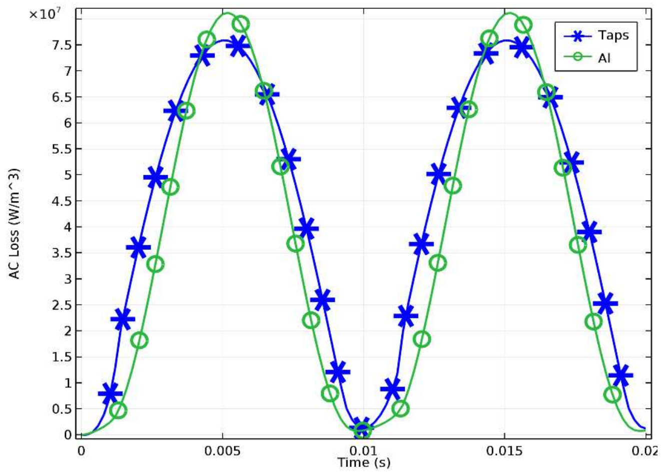

- Only one duct is fil with 15 SPI taps, SUN taps and 3 stainle steel taps, and the rest the four ducts are filled with 30 stainle steel taps.
- Three SPI taps (Tap 12, 14) and three SU taps (Tap 19, 23, 25) a extracted from the cab for clear plot. The resu agree well with t experimental results.
- AC loss always increas with cable current a increases as the numb of taps increases.

ctro-mechanical-thermal behavior of TSSC HTS CICC

stribution of von Mises stress （electromagnetic stress ）

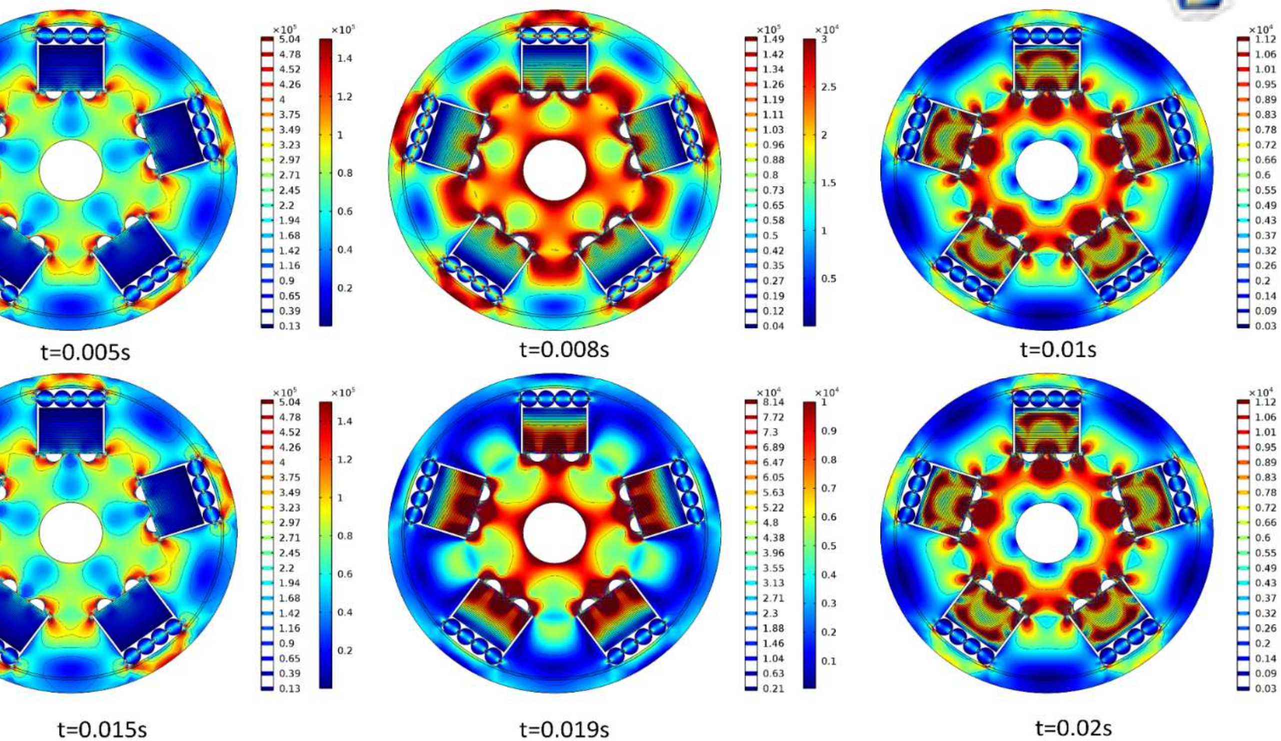

Distribution of von Mises stress (color chat) caused by Lorentz force on the middle cross section of cable at different time points

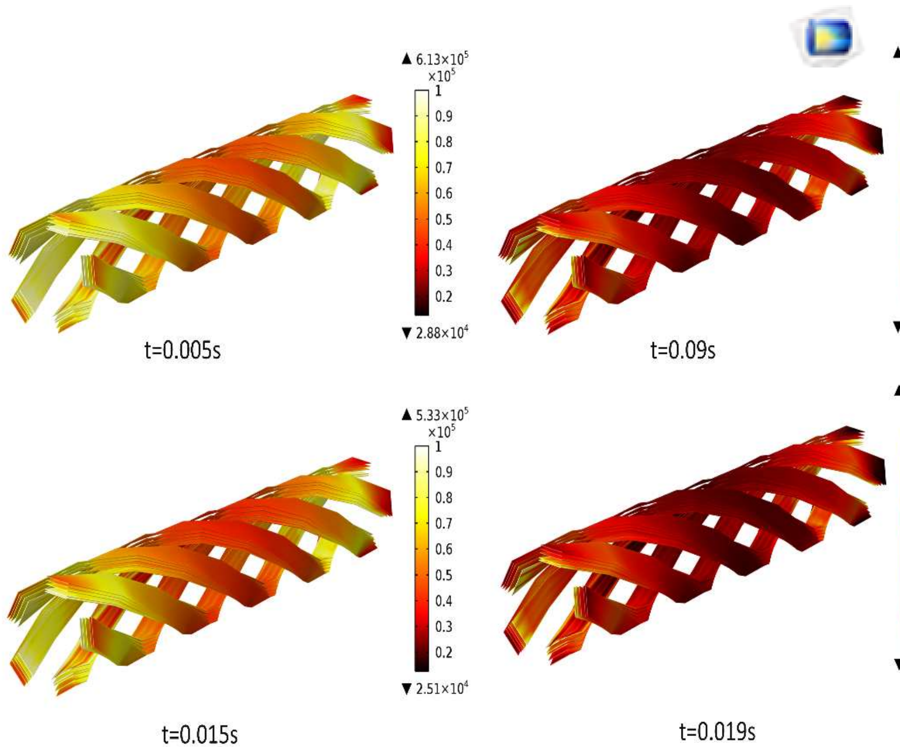

Distribution of von Mises stress caused by Lorentz force in the taps of cable at different time points

- The maximum stress occurs at the edge of ducts and semicircular grooves due to the stress concentration effect, and the stress in two ends are higher than in middle cross section.
- The stress vary with time, which consistent with the change of the transport current.

tro-mechanical-thermal behavior of TSSC HTS CICC

The Lorentz force in taps increase with the position *y*, which consistent with the magnetic fie distribution.

The stress in taps decrease with the position *y* and the discontinuity stress is caused by stress concentrati

The Lorentz force in taps is higher than Al core, but the stress in taps is lower in Al core.

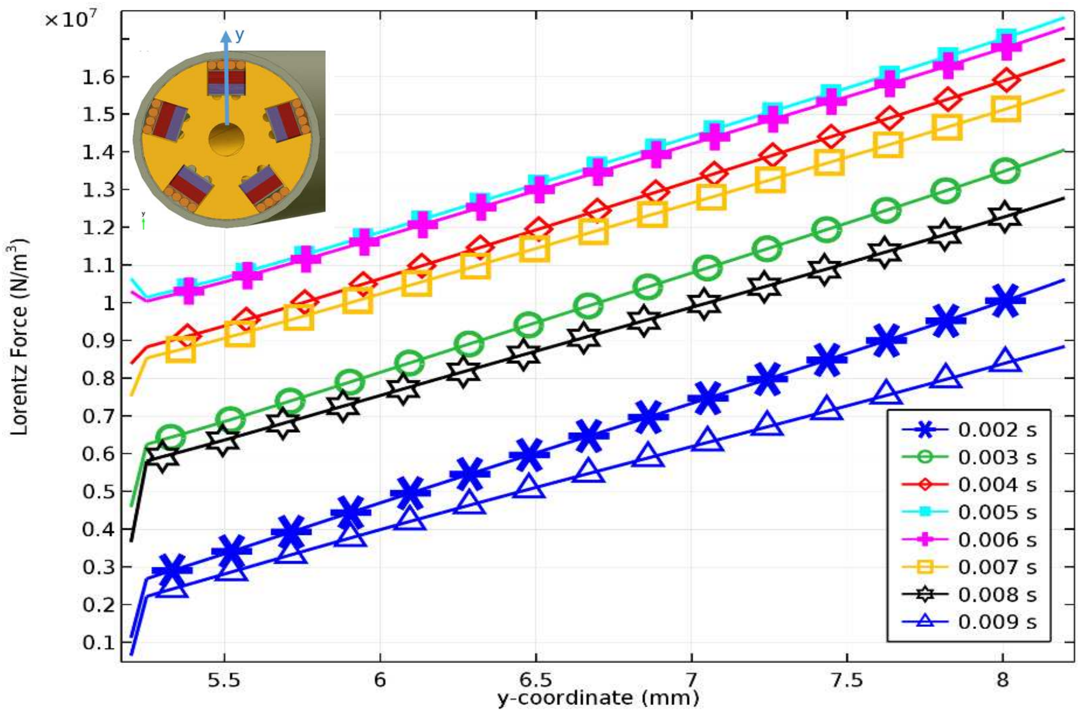

Distribution of Lorentz force

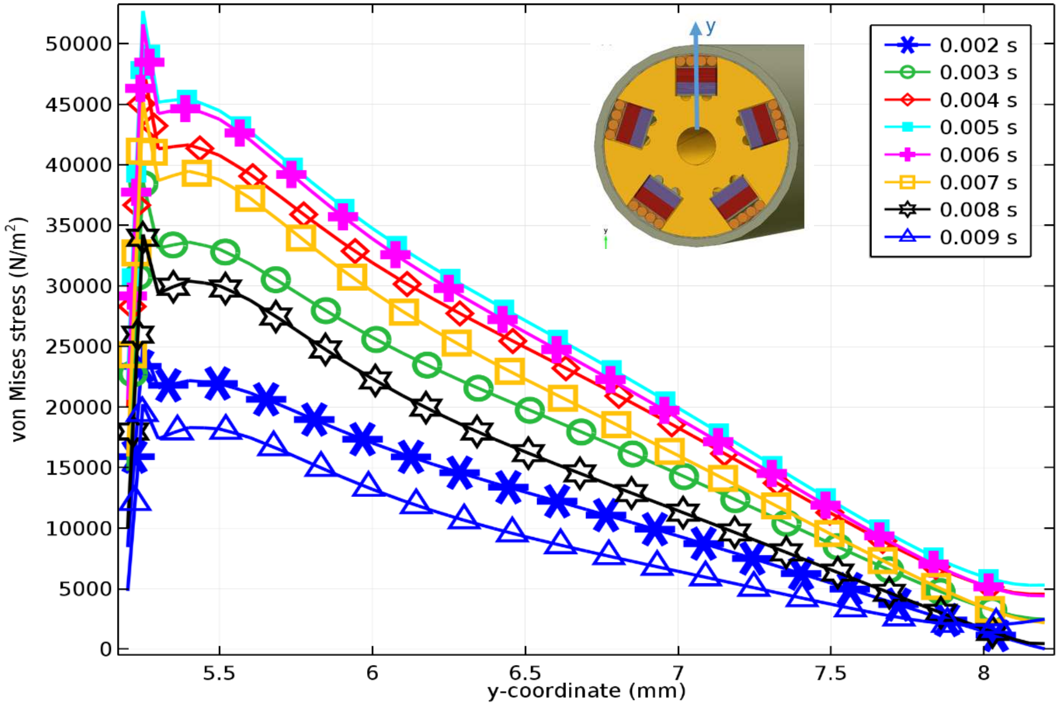

Distribution of von Mises stress

ctro-mechanical-thermal behavior of TSSC HTS CICC

mperature distribution

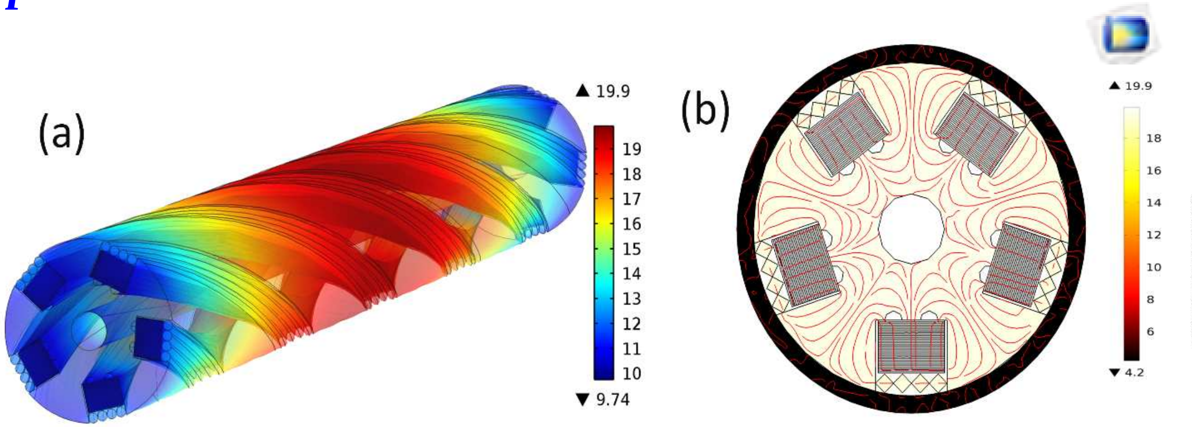

(a) The temperature distribution of the cable before cooldown. (b) The heat flux distribution on the middle cross section of cable before cooldown.

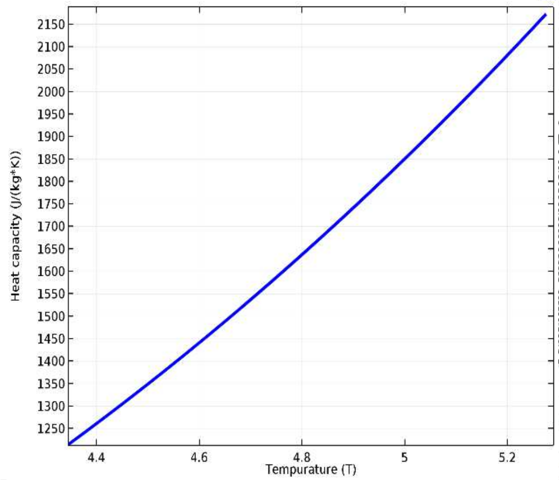

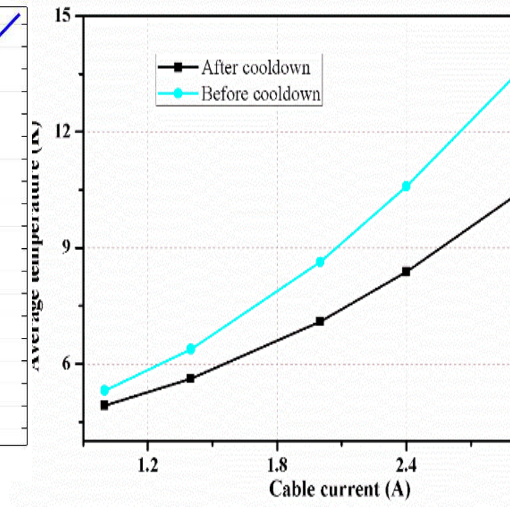

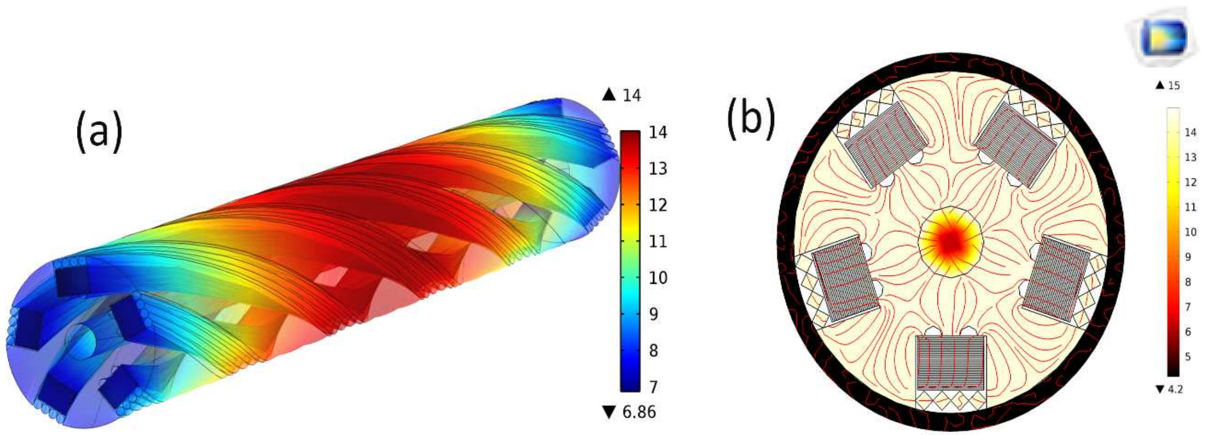

(a) The temperature distribution of the cable after cooldown. (b) The heat flux distribution on the middle cross section of cable after cooldown.

- In the case of cooling, heat flux exchanges between liquid helium and cable core.
- Cooling has a significant effect on the temperature distribution. It can reduce the temperature of the cable.

ctro-mechanical-thermal behavior of TSSC HTS CICC

mperature distribution

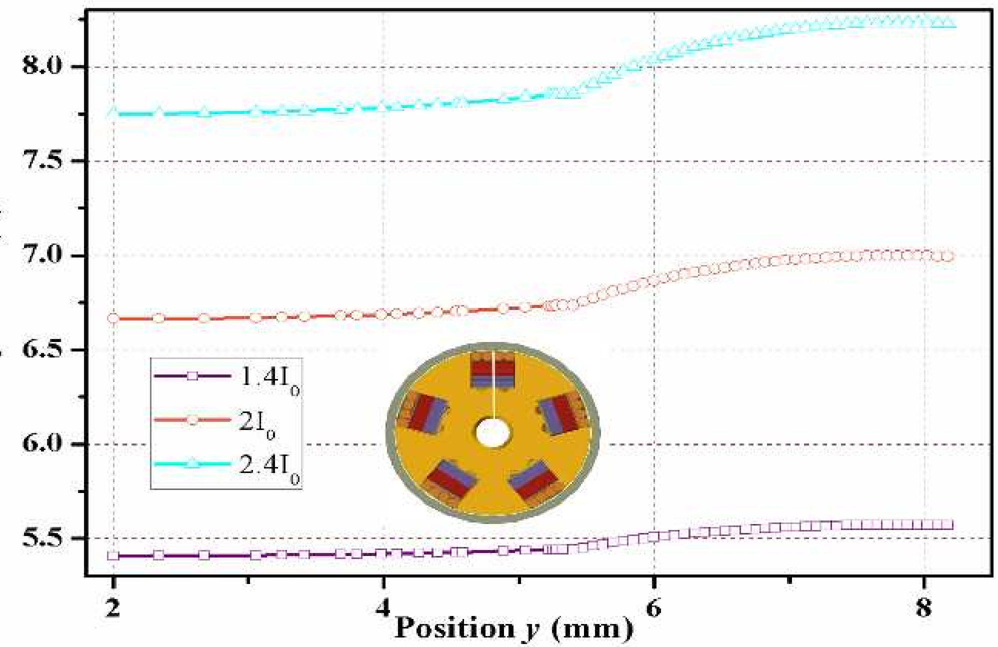

The temperature distribution in the extracted line on the middle cross section of the cable before cooling.

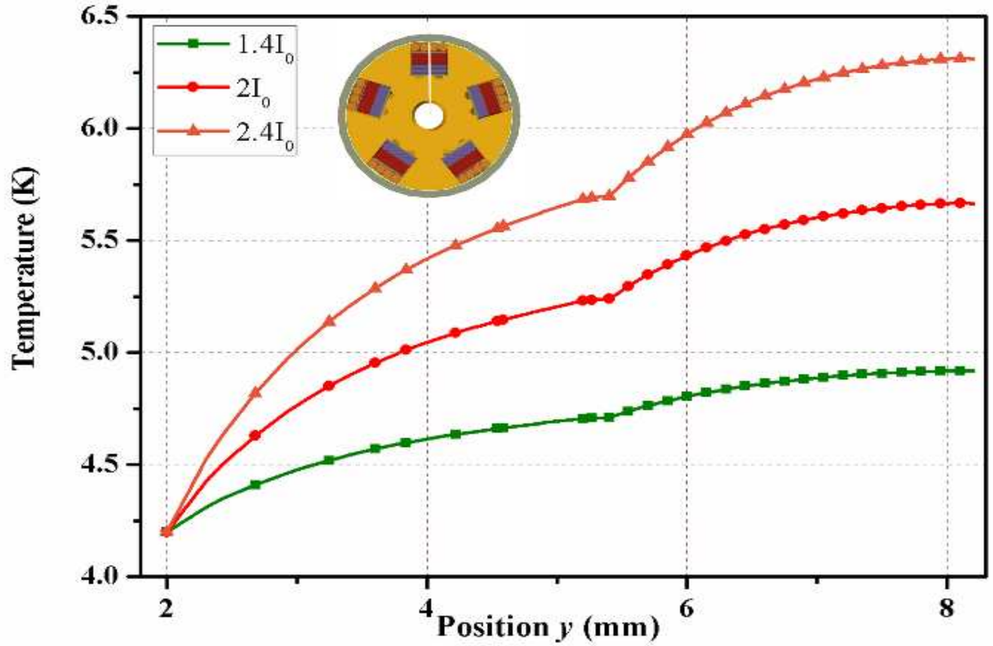

The temperature distribution in the extracted line on the middle cross section of the cable after cooling.

- The temperature in metal matrix and taps increase with the position *y*. Temperature discontinuities in figures are the junctions of the matrix and taps.
- The cable temperature increase obviously with the transport current increase. This is because the current increases led to an increase in the Joule heat.

ctro-mechanical-thermal behavior of TSSC HTS CICC

hermal stress distribution

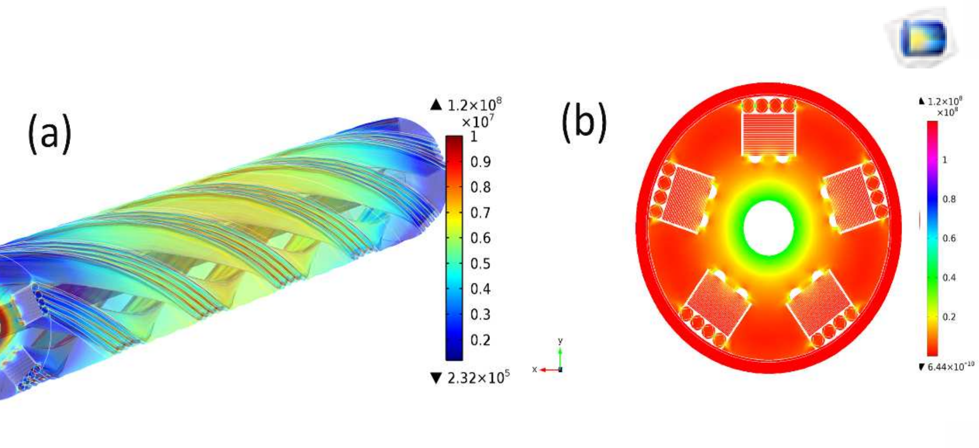

) The thermal stress distribution of the cable before cooling. (b) The thermal stress distribution on the middle cross section of cable before cooling.

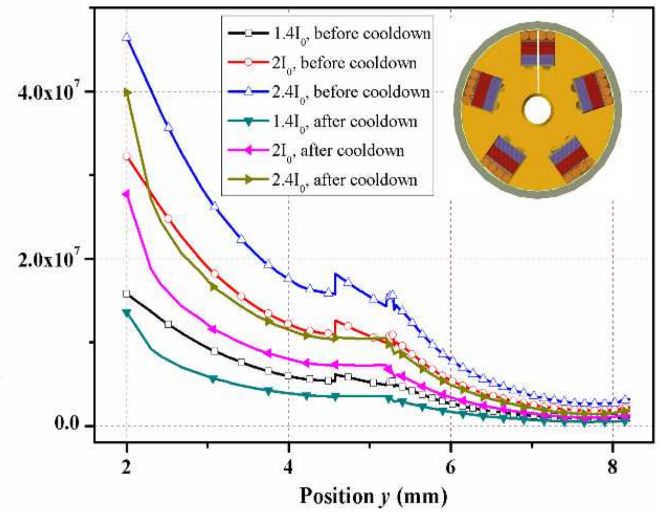

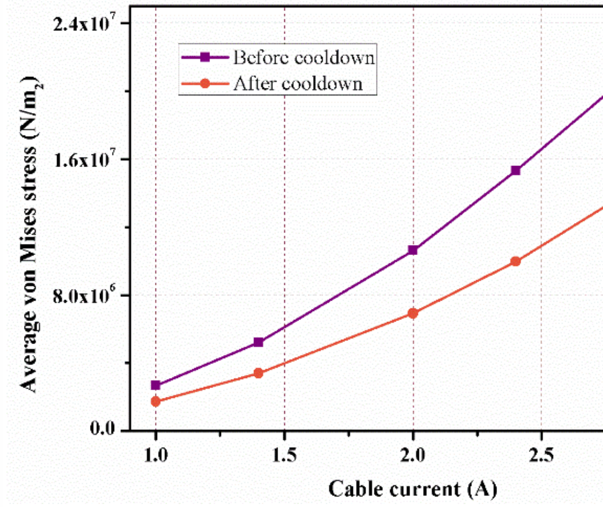

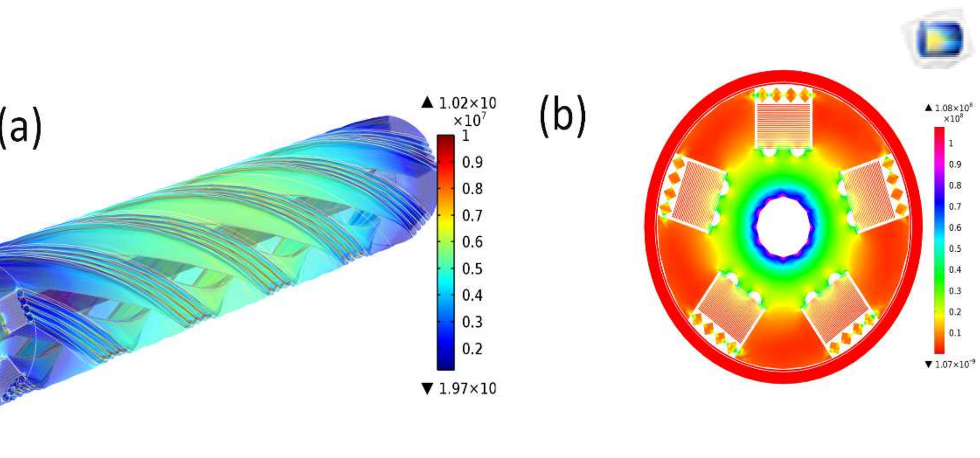

The thermal stress distribution of the cable after cooling. (b) The thermal stress distribution on the middle cross section of cable after cooling.

- The stress level in metal core is higher than that superconducting taps.
- With the change in position y, the stress gradually decreases.
- The Al core bear the main thermal load.
- Excessive thermal stress will squeeze superconducting ta resulting in degradation of superconducting performance cable.
- Selecting the material with low thermal expansion coeffic as the cable core is essential.

Conclusions

TSTC cable:

- **The profiles of displacement, stress and axial strain of TSTC cable under tension and radial compression are computed.**
- **The critical current decreases with increasing load and the plastic deformation makes the degradation more obvious. the longer of the twist pitch of cable, the smaller the degradation of critical current.**

TSSC cable:

- **The transport current is non-uniformly distributed among the TSSC cable, and decrease from the top tape in the stack to the bottom.**
- **Cooling can reduce the temperature of the cable significantly. the cable temperature and stress increase obviously with the transport current increase.**
- **Excessive thermal stress will squeeze superconducting tapes, resulting in degradation of superconducting performance of cable. So, selecting the material with low thermal expansion coefficient as the cable core and improving the cooling efficiency are essential.**


Thanks for your attention！